Multi-Objective Optimization of Distribution Networks via Daily Reconfiguration

Seyed-Mohammad Razavi, *Student Member, IEEE,* Hamid-Reza Momeni, *Senior Member, IEEE,* Mahmoud-Reza Haghifam, *Senior Member, IEEE,* and Sadegh Bolouki, *Member, IEEE*

***Abstract*—This paper presents a comprehensive approach to improve the daily performance of an active distribution network (ADN), which includes renewable resources and responsive loads (RLs), using distribution network reconfiguration (DNR). The optimization objectives considered in this work can be described as (i) reducing active losses, (ii) improving the voltage profile, (iii) improving the network reliability, and (iv) minimizing the operation costs. The proposed approach also accounts for the probability of renewable resource failure given the information collected from their initial state at the beginning of each day. Furthermore, solar radiation variations are estimated based on past historical data, and the impact of the performance of renewable resources such as photovoltaics (PVs) is determined hourly based on a Markov model. Since the number of reconfiguration scenarios is very large, stochastic DNR (SDNR) based on the probability distance method is employed to shrink the scenarios set, before a self-adaptive modified crow search algorithm (SAMCSA) is introduced to find an optimal scenario. Finally, the IEEE 33-bus radial distribution system and the 86-bus Taiwan Power Company (TPC) system are investigated as two case studies to verify the effectiveness of the proposed method.**

***Index Terms*—Distribution network reconfiguration, probability distance, dynamics reconfiguration, crow search algorithm.**

NOMENCLATURE

ω, Ω	Index and set of scenarios.
t, T	Index and set of time intervals.
g, G	Index and set of DGs.
l, L	Index and set of RLs.
es, ESS	Index and set of ESS.
i, j, N_{bus}	Indices and total number of buses.
br, N_{br}	Index and total number of branches.
re	Index of renewable resources.
N_s	Total number of MCS.
ρ^{Grid}	Wholesale electricity price.
SU, SD	Start-up and shut-down costs of DGs.
ρ^{RL}	Contract price of RLs.
$L_{i,t}$	Active power of load i at time t.
R_{br}	Resistance of branch br.
$P_{g,\max}$	Maximum active power of DG g.
$P_{g,\min}$	Minimum active power of DG g.
$Q_{g,\max}$	Maximum reactive power of DG g.
Z, F	Binary variables for DGs' status.
$I_{br,\max}$	Maximum apparent capacity of branch br.
λ, μ	Failure and repair rates of each renewable resource.
$P_{l,\max}$	Maximum active power contributed to RL l.
ρ^{SW}	Price of switching.
P_{re}^{D}	Probability for unavailability of re.
P_{re}^{U}	Probability for availability of re.
$f(X)$	Objective function.
X	Control vector.
$B_{p,i}$	Best position of crow i.
fl_i	Flight length of crow i.
AP_i	Awareness probability of crow i.
IAP_i	Improved awareness probability of crow i.
$C_{op,es}$	ESS operation cost.
$C_{M,es}$	ESS maintenance cost.
P_{es}	Electrical storage power in unit time.
P_{grid}, Q_{grid}	Active and reactive power received from the grid.
P_g, Q_g	Active and reactive power received from DG g.
P_{re}	Active power received from re.
η_l	Maximum demand control coefficient of RL l.
P_l, Q_l	Active and reactive power controlled from RL l.
$V_{i,\max}, V_{i,\min}$	Maximum and minimum voltage of node i.
P_i, Q_i	Active and reactive power loads of node i.
η_{es}	Charging and discharging system efficiency.
P_{es}^{-}, P_{es}^{+}	Charging and discharging ESS in unit time.
SOC_{es}	State of charging in ESS.
$C_{es,\max}$	Maximum capacity of the ESS.
$SOC_{es,\min}$	Minimum state of charging in ESS.
L_i	Load connected to the node i.

S.-M Razavi, H.-R Momeni, M.-R. Haghifam and S. Bolouki are with Department of Electrical and Computer Engineering, Tarbiat Modares University, Tehran 14155-143, Iran e-mails: mohammad_razavi@modares.ac.ir, momeni_h@modares.ac.ir, haghifam@modares.ac.ir, bolouki@modares.ac.ir.

I. INTRODUCTION

TODAY conventional energy sources such as oil, gas, and coal together supply over 80% of the world's primary energy. These fossil fuels contain a large amount of carbon, which is the leading cause of climate change and global warming [1]. Climate change, persistent environmental pollution, and energy crises have led many countries to use renewable energy instead of fossil fuels [2]. Challenges of managing traditional distribution systems have become more complex with the inclusion of distributed generations (DGs) such as PVs, since distribution system management (DSM) should now also account for the uncertain energy production of these resources [3].

A remarkable DSM approach to address these novel challenges is to reconfigure the distribution network. Distribution network reconfiguration (DNR) is carried out by changing the cosmetic structure of a distribution network by the status of tie and sectionalizing switches. DNR methods are divided into static and dynamic categories [4]. Static reconfiguration methods are those that are often performed on annual, seasonal, or monthly bases, while dynamic reconfiguration involves short periods of time, such as daily or hourly periods [4]. Renewable resources may experience failure in different parts of their components [5]. Such failures are of great importance since renewable resources are responsible for a significant portion of the generated energy in the network. In this work, we propose an efficient dynamic reconfiguration scheme, that is free of remotely controlled switches and takes into account the possibility of failure of the renewable farms.

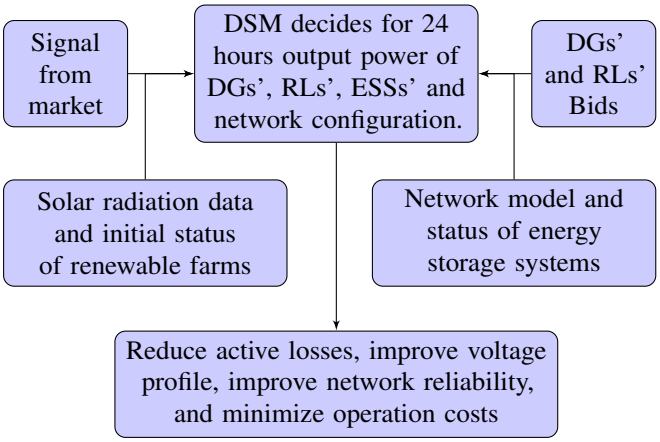

Figure 1: Block diagram of the proposed work.

A. Literature Review

The primary purpose of reconfiguration in the literature has been minimizing network losses [6], [7]. However, other objectives such as balancing load demand and improving reliability indicators have also been addressed [8], [9]. Over the past two decades, numerous methods have been proposed to address the DNR problem, a survey of which can be found in [10]. The uncertainty of generation and load demand is one of the critical factors that must be taken into consideration for DNR [11]. In [12], the uncertainty involved in renewable sources is modeled by 24-hour scenarios and, for each hour, an optimal configuration with respect to the balance between generation and demand is presented. In [13], accounting for the uncertainty of renewable generation, the DNR problem is examined in three stages, the evaluation stage, the time division stage, and the optimization stage. Taking the consumers' daily load curves into account, [14] conducts DNR aiming to reduce active losses. In [15], the daily load demand is factored in DNR to improve reliability indices. DNR is carried out in [16] considering the spatial and temporal capabilities of autonomous electric vehicles, and their demand for charging. There, a mixed-numeric programming model is proposed to make DNR compatible with charging and discharging of electric vehicles. Authors in [17] investigate the DNR problem with the aim of increasing DG penetration capacity given thermal and voltage constraints and direct values of consumer demand at different times. Risk-based reconfiguration is suggested in [18], which considers load and generation uncertainty and employs reward/penalty schemes. In [19], the two-point estimation method is used to incorporate uncertainty into the analysis. Authors in [20] propose a multi-period DNR model to take the dynamic load demand into account. The daily DNR problem is then solved using the genetic algorithm (GA) method to minimize the total network losses by considering the optimal DG output over the next 24 hours. In [21], a method for determining the minimum network losses with uncertain load and renewable generation is presented. In particular, a mixed-integer two-stage robust optimization formulation and a decomposition algorithm are proposed to address the problem.

B. Contributions

Current solutions to the DNR problem generally have high computational complexities, which highlights the need for new, more efficient methods. In distribution networks with consistent changes in generation and demand and the possibility of failure of various equipment types, it is imperative to find quick solutions to achieve satisfactory results. Equipment failure negatively impacts DSM, which aims to improve the welfare of consumers and increase the profits of the distribution companies. Table I compares the existing reconfiguration methods with the one proposed in this work. Major contributions of the paper are described below.

1) Our DNR method takes equipment failure into consideration, which is one of the most important issues in DSM as it can greatly impact the network's performance. Our focus is on the failure of part of the PV farm that reduces its penetration in the network during the repair period. An optimal reconfiguration sequence is introduced according to the operating horizon (e.g., 24 hours). As a result, if the PV penetration increases along the planning horizon (repairing a failure part), the objective functions such as active losses, voltage deviations, and operating costs will deviate from their desirable values. DSM then tries to change the network configuration in such a way that the objective functions continue to be optimized by increasing the PV farm penetration. As demonstrated in Figure 1, the effects of the possibility of failure of renewable farms such as PV with uncertainty in solar radiation and the impact of DGs, responsive loads (RLs), and energy storage systems (ESSs) on the result of DNR are explicitly investigated.

2) Dynamic reconfiguration often requires high computational speed and the personnel's fast performance. Moreover, most of the existing literature on dynamic reconfiguration assumes that switches can be controlled remotely, which is not always practical since these switches are costly to install and control [4], [22]. In this work, hourly optimal configurations for the next 24 hours is selected at the beginning of each day, which provides the personnel ample time to change the status of the switches and eliminates the need for remotely controlled switches. Furthermore, to reduce the computational complexity, an efficient stochastic DNR method is proposed.

Table I: Comparing DNR methods

Reference	Approach		Possibility of failure	Methodology
	static	dynamic		
[9]	✓	×	×	DPSO
[11]	×	✓	×	GA
[13]	×	✓	×	HPSO
[16]	×	✓	×	MIP
[17]	×	✓	×	MP-OPF
[18]	✓	×	×	PSO
[19]	✓	×	×	MBA
[23]	✓	×	×	MILP
[26]	✓	×	×	HSA
[27]	✓	×	×	APSO
This work	×	✓	✓	SAMCSA

3) In deriving static or dynamic reconfiguration, a variety of methods have been employed, including mathematical programming, such as mixed-integer linear programming [23], mixed-integer conic programming [24], and mixed-integer quadratically constrained programming [25], and metaheuristic techniques, such as GA [20], harmony search algorithm (HSA) [26], and adaptive particle swarm optimization (APSO) [27]. In this work, the so-called self-adaptive modified crow search algorithm (SAMCSA) is introduced as part of the solution to the reconfiguration problem.

C. Paper Organization

The remainder of the paper is organized as follows. In Section II, the optimization objective function is formulated. Section III explores uncertainty of renewable resources by introducing a decision tree derived from resource failure and random behavior of solar radiation. The multi-objective optimization and the SAMCSA method are presented in Sections IV and V, respectively. Section VI presents two case studies and the results obtained with the proposed analytical reconfiguration algorithm. Finally, Section VII concludes the paper with a summary and future directions of this research.

II. Formulation of Multi-objective DNR

The decision variable X for the DNR problem is a vector consisting of the tie and sectionalizing switches, the DGs, the RLs contract, and the ESSs, i.e.,

$$\begin{aligned}
\mathbf{X} &= \left[\overline{\mathbf{Tei}}, \overline{\mathbf{SW}}, \overline{\mathbf{DG}}, \overline{\mathbf{RL}}, \overline{\mathbf{ESS}}\right], \\
\overline{\mathbf{Tei}} &= (Tei_1, Tei_2, \ldots, Tei_n), \\
\overline{\mathbf{SW}} &= (SW_1, SW_2, \ldots, SW_n), \\
\overline{\mathbf{DG}} &= (DG_1, DG_2, \ldots, DG_n), \\
\overline{\mathbf{RL}} &= (RL_1, RL_2, \ldots, RL_n), \\
\overline{\mathbf{ESS}} &= (ESS_1, ESS_2, \ldots, ESS_n).
\end{aligned} \tag{1}$$

A. Multi-objective Function

Based on the information received from the initial state of renewables at the time of optimization, the four-dimensional objective function $\mathbf{OF}(\mathbf{X})$ is described as

$$\mathbf{OF}(\mathbf{X}) = [OF_1(\mathbf{X}), OF_2(\mathbf{X}), OF_3(\mathbf{X}), OF_4(\mathbf{X})]', \tag{2}$$

where reliability, active losses, voltage deviation, and operating costs are the first to fourth parts of the objective function, respectively. These functions are briefly described below in that order.

$OF_1(X)$ represents the probability of hourly failure of the branches, which is an indicator for determining the reliability of the load point. Using the Monte Carlo simulation method, the probability of failure at distribution branches for hourly timing is modeled. The availability of branches per hour is determined by failure time t_F and repair time t_R calculated as [28]

$$t_F = -MTTF.\ln(u_1),\ t_R = -MTTR.\ln(u_2), \tag{3}$$

where $MTTF$ and $MTTR$ are the mean failure time and the mean repair time, respectively, and u_1 and u_2 are random variables that are uniformly distributed between 0 and 1. Values t_F and t_R are rounded to the nearest integer. The procedure continues by generating new values for u_1 and u_2 until the entire time period ($N_{tp} = 8760$ hours) is covered, which is introduced as one of the Monte Carlo simulation scenarios (N_s) [28]. For the branch br with scenario s, we define the variable $a_{br,s}$ to be equal to 1 at range t_F and 0 at range t_R. The probability of hourly failure of each branch is then defined by the matrix Re^t_{br} as

$$Re^t_{br} = \begin{bmatrix} a^1_{1,1} \cdots a^{8760}_{1,1}, & \cdots & a^1_{1,N_s} \cdots a^{8760}_{1,N_s} \\ \vdots & \ddots & \vdots \\ a^1_{N_{br},1} \cdots a^{8760}_{N_{br},1}, & \cdots & a^1_{N_{br},N_s} \cdots a^{8760}_{N_{br},N_s} \end{bmatrix}. \tag{4}$$

A time instant t is calculated by generating a random number between 0 and 1 multiplied by N_{tp}. The probability of failure of the branch br is equal to the ratio of sum $a^t_{br,s}$ to the number of scenarios N_s. The failure probability of any configuration is as follows:

$$OF_1(X) = \sum_{i=1}^{N_{br}} L_i \left(\frac{\sum_{s \in S} a^t_{br,s}\, x_{br}}{N_s} \right), \tag{5}$$

where x_{br} is a binary variable representing the active and inactive branch and N_s is the number of scenarios implemented in the Monte Carlo simulation. One notices that the Monte Carlo simulation is performed for all the branches before the optimization process begins and only the matrix Re^t_{br} is used in the optimization. This means that the computation time of the Monte Carlo simulation does not affect optimization.

$OF_2(X)$ represents active losses in the network and is expressed as

$$OF_2(X) = \sum_{br \in N_{br}} R_{br} \left| I_{br} \right|^2. \tag{6}$$

$OF_3(X)$ represents of voltage deviation in each node, i.e.,

$$OF_3(X) = \max\left[\left| v_{ref} - \min v_i \right|, \left| v_{ref} - max\ v_i \right| \right]. \tag{7}$$

Finally, $OF_4(X)$ represents the distribution network operation costs, including the cost of electricity purchased from the grid, the cost of energy generated by DGs, the cost of switching,

the cost of using RLs, and the cost of using ESSs, i.e.,

$$OF_4(X) = C_{Grid} + C_{DG} + C_{RL} + C_{SW} + C_{ESS}, \quad (8)$$

where

$$C_{Grid} = \rho^{Grid} P_{Grid}, \quad (9)$$

$$C_{DG} = \sum_{g\in G} C_g + \sum_{g\in G} Z_g SU_g + \sum_{g\in G} F_g SD_g, \quad (10)$$

$$C_{SW} = \rho^{SW} \sum_{br\in N_{br}} \left| X_{br,t} - X_{br,t-1} \right|, \quad (11)$$

$$C_{RL} = \sum_{l\in L} \rho^{RL} P_l^{RL}, \quad (12)$$

$$C_{ESS} = \sum_{es\in ESS} C_{op,es} P_{es} + C_{M,es}. \quad (13)$$

Equations (9)-(10) represent energy purchased from the grid and the cost of using DGs, respectively [29], [30]. Here, C_g is calculated as $a_g U_g + b_g P_g + c_g P_g^2$, where a, b, and c are cost function coefficients. SU_g and SD_g are the start-up and shut-down costs of DG g, respectively. Equation (11) is the cost of switching [31], (12) is the cost of power outages for consumers in RLs [30], and (13) represents the cost of using ESSs [32].

B. Electrical Constraints and Limits

The constraints used in the DNR problem are as follows:

$$\begin{aligned} &P_{grid} + \sum_{g\in G} P_g + \sum_{re\in RE} P_{re} + \sum_{l\in L} P_l + \sum_{es\in ESS} \eta_{es} \left(P_{es}^{-} - P_{es}^{+} \right) \\ &= \sum_{i\in N_{bus}} P_i + \sum_{i\in N_{bus}} V_i V_j Y_{ij} \cos(\theta_{ij} - \delta_i + \delta_j), \end{aligned} \quad (14)$$

$$\begin{aligned} &Q_{grid} + \sum_{g\in G} Q_g + \sum_{l\in L} Q_l \\ &= \sum_{i\in N_{bus}} Q_i + \sum_{i\in N_{bus}} V_i V_j Y_{ij} \sin(\theta_{ij} - \delta_i + \delta_j), \end{aligned} \quad (15)$$

$$V_{i.\min} \le V_i \le V_{i.\max}, \; V_{\text{slack}} = 1, \quad (16)$$

$$\begin{aligned} &P_{g,\min} \le P_g \le P_{g,\max}, \\ &Q_{g,min} \le Q_g \le Q_{g,max}, \end{aligned} \quad (17)$$

$$\begin{aligned} &SOC_{es} = SOC_{es,t-1} + \eta_{es} \left(P_{es}^{-} - P_{es}^{+} \right), \\ &SOC_{es,min} \le SOC_{es} \le C_{es,\max}, \end{aligned} \quad (18)$$

$$\begin{aligned} &N_{br} = N_{bus} - 1, \\ &\left(I + M_G \right)^{N_{bus}-1} > 0, \end{aligned} \quad (19)$$

$$\begin{aligned} &0 \le P_l \le P_{l,\max}. \left(\eta_{t,l}/100 \right), \\ &\eta_{t,l} \le \eta_l - \sum_{t'=1}^{t-1} \eta_{t',l}, \end{aligned} \quad (20)$$

$$|I_{br}| < I_{br,\max}, \quad (21)$$

$$\sum_{t=1}^{24} |X_{br,t} - X_{br,t-1}| \le N_{br,\max}. \quad (22)$$

Equations (14) and (15) represent the active and reactive power load flow; (16) represents the voltage constraints; (17) represents the active and reactive power limits of DGs; and (18) shows the charging and discharging limits of storages. Equation (19) represents the topology constraints, where M_G is the adjacency matrix of the selected configuration (G) and the inequality is to be understood element-wise. This constraint guarantees that in the selected configuration all points are connected to the slack node. The major limitation in switching is that the structure of each configuration must remain radial. Equation (20) represents the RLs' constraints. According to the agreement between some consumers and DSM, energy consumption can be reduced to a limited extent. Equation (21) represents the flow capacity of the branches, and finally, (22) represents the maximum number of switching allowed for a switch.

III. Scenario Generation and Reduction

Since DNR algorithms often involve a high computational complexity, other concurrent issues such as equipment failure tend to be overlooked. In this paper, we discuss possibility of failure of renewable resources and uncertainty in solar radiation simultaneously. Due the very large number of scenarios, we should also carefully reduce the set of scenarios, leading us to the so-called SDNR problem.

A. Scenario Generation for Initial PV Status

In this work, it is assumed that each PV farm consists of T equipment items. The power output of a PV farm is equal to the sum of the power outputs of all the items. If repairs and failures of an equipment item are exponentially distributed, according to the Markov chain model, its unavailability probability $\left(P_{re}^{D}\right)$ and availability probability $\left(P_{re}^{U}\right)$ at t are defined as [33]

$$P_{re}^{D}(t) = \frac{\lambda_{re}}{\mu_{re} + \lambda_{re}} + \left(P_{re}^{D}(0) - \frac{\lambda_{re}}{\mu_{re} + \lambda_{re}} \right) e^{-(\mu_{re} + \lambda_{re})t}, \quad (23)$$

$$P_{re}^{U}(t) = \frac{\mu_{re}}{\mu_{re} + \lambda_{re}} + \left(P_{re}^{U}(0) - \frac{\mu_{re}}{\mu_{re} + \lambda_{re}} \right) e^{-(\mu_{re} + \lambda_{re})t}, \quad (24)$$

where λ_{re} and μ_{re} are the failure rate and repair rate of each equipment item, respectively. In dynamic reconfiguration, unlike static reconfiguration, the value t is very small, meaning that the second term in the right hand expressions of (23) and (24) cannot be omitted. Figure 2 shows an overview of the proposed method. If part of the equipment is unavailable at time

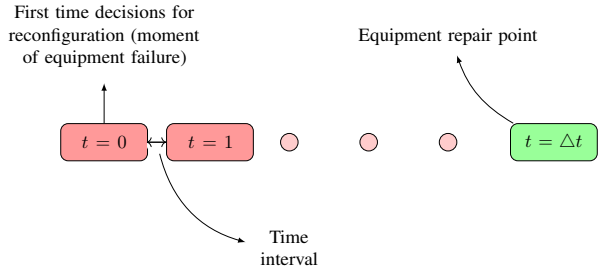

Figure 2: Model overview for the availability or unavailability of PV farm equipment.

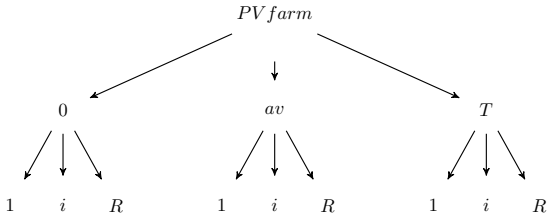

Figure 3: Decision tree diagram for a solar farm

$t=0$, the probability equation of the number of equipment available at the time $\triangle t$ is as [33]

$$\pi_{av}=\sum_{\substack{i=0\\ i\leq T-A\\ i\geq av-A}}^{av}\binom{T-A}{i}\binom{A}{av-i}P_{U0}^{U_t^i}\times P_{D0}^{U_t^{av-i}}\times P_{U0}^{D_t^{T-A-i}}\times P_{D0}^{D_t^{A-av+i}}, av=0,...,T, \quad (25)$$

where av is the number of available items at time $t=\triangle t$, and A is the number of unavailable items at $t=0$. The probability matrix for 24 hours can now be defined as

$$\begin{bmatrix}\pi_{1,0} & \cdots & \pi_{1,T}\\ \vdots & \ddots & \vdots\\ \pi_{24,0} & \cdots & \pi_{24,T}\end{bmatrix}. \quad (26)$$

B. Scenario Generation for Solar Irradiance

In the literature, by collecting past historical data, solar radiation is modeled using the Beta distribution for each hour of the day [34]–[36], which is as

$$f_s^t(S)=\begin{cases}\frac{\Gamma(\alpha^t+\beta^t)}{\Gamma(\alpha^t)\Gamma(\beta^t)}S^{(\alpha^t-1)}(1-S)^{(\beta^t-1)} & 0\leq S\leq 1,\ \alpha,\beta\geq 0\\ 0 & \text{otherwise,}\end{cases} \quad (27)$$

where α and β are positive constants calculated as [36]

$$\beta=(1-\mu)\left(\frac{\mu(1+\mu)}{\sigma^2}-1\right),\ \alpha=\frac{\mu\times\beta}{1-\mu}, \quad (28)$$

where μ and σ are the mean and standard deviation from historical data, respectively. In the past, only one random variable was considered and, by comparing it to the cumulative distribution function (CDF), solar radiation would be estimated. However, here we produce a larger set of random variables to increase the computational accuracy. The probability of each sample is $\pi_i=n_i/N,\ i=1,\ldots,R$, where N and n_i are the total number of samples and the number of repetitions of sample i, respectively. Hence, the probability of solar radiation operational horizon (e.g., 24 hours) is expressed as

$$\begin{bmatrix}\pi_{1,0} & \cdots & \pi_{1,R}\\ \vdots & \ddots & \vdots\\ \pi_{24,0} & \cdots & \pi_{24,R}\end{bmatrix}. \quad (29)$$

C. Scenario Reduction

According to the scenarios related to the initial state and solar radiation using stochastic programming, a decision tree, similar to that of Fig. 3, can be formed with three layers and $N_\Omega=TR$ scenarios. One notices that it could be difficult to use this method to solve a daily optimization problem since it is not scalable, meaning that increasing the number of scenarios will significantly increase the computation time. Therefore, we employ a probabilistic distance method to reduce the number of scenarios. The most common probability distance utilized in stochastic programming is the Kantorovich distance [28]. First, function ν is defined as the norm of the difference between pairs of scenarios [28], that is

$$\nu(\omega,\omega')=\|r(\omega)-r(\omega')\|, \qquad \forall\omega\in\Omega, \quad (30)$$

where $r(.)$ is the outcome of each scenario at each step of the decision tree. The values of function ν can be conveniently arranged into a symmetric matrix with zeros as the diagonal elements, where each row (and column) represents a scenario. We now perform an iterative algorithm starting with the set of all possible scenarios $\Omega_j=\{1,2,\ldots,N_\Omega\}$. We find the scenario (ω_s) within Ω_j, which has the minimum aggregated distance to other scenarios in Ω_j [28], that is

$$d_\omega=\sum_{\omega'=1,\omega'\neq\omega}^{N_\Omega}\pi_{\omega'}\nu(\omega,\omega'),\ \forall\omega\in\Omega_j,$$
$$\omega_s\in\arg\min_{\omega\in\Omega_j}\ d_\omega. \quad (31)$$

We then update values of the matrix and remove ω_s from the set Ω_j of scenarios, i.e.,

$$\nu(\omega,\omega')=\min\{\nu(\omega,\omega'),\nu(\omega,\omega_s)\},\ \forall\omega,\omega'\in\Omega_j,$$
$$\Omega_j^*=\Omega_j\backslash\omega_s. \quad (32)$$

After a number of iterations, the set $\Omega_s^*=\Omega\backslash\Omega_j^*$ is selected as the set of preferred scenarios. Redistribution of probabilities can be accomplished as follows. The probabilities of selected scenarios $\omega\in\Omega_s^*$ are computed as

$$\pi_\omega^*\longleftarrow\pi_\omega+\sum_{\omega'\in J(\omega)}\pi_{\omega'}, \quad (33)$$

where

$$J(\omega)=\left\{\omega'\in\Omega_j^*\,|\,\omega=\arg\min_{\omega''\in\Omega_s^*}\nu(\omega'',\omega')\right\}. \quad (34)$$

The method of reducing the scenario described above is known as the fast forward selection algorithm [28]. The pseudo-code for the fast forward selection algorithm is given in Algorithm 1.

Algorithm 1 Fast forward selection

Compute function $\nu^{[0]}(\omega, \omega')$ for each pair of scenarios ω and ω' in Ω.
Set $\Omega_j^{[0]} = \{1, 2, \ldots, N_\Omega\}$
for $i = 1$ to i_{Max} **do**
  Compute d_ω^i
  Select $\omega_i \in \arg\min_{\omega \in \Omega} \ d_\omega^{[i]}$
  Set $\Omega_j^{[i]} = \Omega_j^{[i-1]} \backslash \omega^{[i]}$
  Update $\nu^{[i]}(\omega, \omega')$
end for
Compute π_ω^*

Since we have considered both equipment failure and solar radiation, a scenario is represented by a pair (av^{ch}, i^{ch}), where av^{ch} indicates the failure scenario and i^{ch} indicates the solar radiation scenario. The selection probabilities of scenario (av^{ch}, i^{ch}) in the operational horizon (e.g., 24 hours) can be represented by the following matrix:

$$\begin{bmatrix} \pi_{av^{ch},i^{ch}}^{1,1} & \cdots & \pi_{av^{ch},i^{ch}}^{1,F} \\ \vdots & \ddots & \vdots \\ \pi_{av^{ch},i^{ch}}^{24,1} & \cdots & \pi_{av^{ch},i^{ch}}^{24,F} \end{bmatrix}. \tag{35}$$

D. Solar Generation

The output power of the solar generator depends on the temperature and the radiation of the sun which are, according to [36], calculated as

$$\begin{aligned} P_{pv_s} &= \gamma \times FF \times V_{ij} \times I_{ij}, \\ T_{ct} &= T_{at} + S \times \left\{ \frac{NOCT - 20}{0.8} \right\}, \\ V_{ij} &= V_{oc} - K_{vt} \times T_{ct}, \\ I_{ij} &= S \times \{ I_{sc} + K_{ct} \times (T_{ct} - 25) \}, \\ FF &= \frac{V_{mp} \times I_{mp}}{V_{oc} \times I_{oc}}, \end{aligned} \tag{36}$$

where P_{pv_s} is the output power at solar irradiance S, γ is the number of solar modules, V_{ij} and I_{ij} are the output voltage and current, T_{ct} and T_{at} are the module temperature and the ambient temperature at which the module is located ($^\circ$C), $NOCT$ is the cell temperature in nominal operation, s is the solar radiation rate, K_{ct} and K_{vt} are the voltage ($V/^\circ$C) and current ($A/^\circ$C) temperature coefficients, V_{mp} and I_{mp} are the maximum voltage and current power point, and finally V_{oc} and I_{oc} are the open-circuit voltage and the short-circuit current, respectively.

IV. Multi-objective Optimization

In general, a multi-objective optimization problem with different constraints can be expressed as

$$\begin{aligned} \min \ \mathbf{OF}(\mathbf{X}) &= [F_1(\mathbf{X}), F_2(\mathbf{X}), \ldots, F_n(\mathbf{X})]' \\ \mathbf{h_i}(\mathbf{X}) &= 0, \ i = 1, 2, \ldots, N_{eq} \\ \mathbf{g_i}(\mathbf{X}) &\leq 0, \ i = 1, 2, \ldots, N_{ueq}, \end{aligned} \tag{37}$$

where $\mathbf{h_i}$ and $\mathbf{g_i}$ are the equality and inequality constraints, respectively. In multi-objective optimization, the objective functions may conflict, leading to inevitable tradeoffs. A solution is said to dominate another solution if it is not worse with respect to any of the objective functions and is better with respect to at least one of the objective functions. Given a multi-objective optimization problem, one often seeks to find a *Pareto optimal solution*, which is a solution that is not dominated by any other solution. More precisely, solution $\mathbf{X}$ dominates solution $\mathbf{Y}$, if

$$\begin{aligned} &\forall j \in 1, 2, \ldots, N_f, F_j(\mathbf{X}) \leq F_j(\mathbf{Y}), \\ &\exists k \in 1, 2, \ldots, N_f, F_k(\mathbf{X}) < F_k(\mathbf{Y}). \end{aligned} \tag{38}$$

Since the DNR problem is a nonlinear optimization problem with equality and inequality constraints, it needs to be converted into an unconstrained one by constructing an augmented objective function incorporating penalty factors for any value violating the constraints, i.e.,

$$\begin{aligned} F_i(X) = f_i(X) &+ p_1 \sum_{j=1}^{N_{eq}} (h_j(X))^2 \\ &+ p_2 \sum_{j=1}^{N_{ueq}} (\max[0, g_j(X)])^2. \end{aligned} \tag{39}$$

Given that the aforementioned functions have different properties, we use fuzzy membership to formulate them on an equal footing, that is

$$\mu f_i = \begin{cases} 1 & f_i(X) \leq f_i^{\min} \\ 0 & f_i(X) \geq f_i^{\max} \\ \frac{f_i^{\max} - f_i(X)}{f_i^{\max} - f_i^{\min}} & f_i^{\min} \leq f_i(X) \leq f_i^{\max}, \end{cases} \tag{40}$$

where f_i^{max} and f_i^{min} are the upper and lower limits of each of the objective functions, respectively, calculated according to the system constraints.

V. Solution Procedure

In this section, the proposed Self-Adaptive Modified Crow Search Algorithm (SAMCSA) is described in detail.

A. Original Crow Search Algorithm (CSA)

The CSA is one of the modern optimization methods introduced by Askarzadeh [37]. This method is inspired by the crows' intelligent behavior in hiding their food to solve an optimization problem. This algorithm provides a simple concept and an effective technique that can be implemented quickly. In this algorithm, the crow i flight length in each iteration is denoted by fl_i, while the degree of awareness of

the crow j pursuit is denoted by the awareness probability AP_j. The pseudo-code for the CSA is given in Algorithm 2.

Algorithm 2 The original CSA

Randomly create the initial position of all the crows (nPop) at random
Evaluate the objective function and determine best position (B_p) for each crow
while $It = It_{Max}$ **do**
  for $i = 1$ *to nPop* **do**
    The crow i randomly selects crow j from the population.
    if $rand_i \geq AP_j$ **then**
      $\mathbf{X}_i^{it} = \mathbf{X}_i^{it-1} + rand_i \times fl_i \times \left(B_{p,j}^{it-1} - \mathbf{X}_i^{it-1}\right)$
    else
      $\mathbf{X}_i^{it} =$ *a random position in the search space*
    end if
  end for
  Check the feasibility of new positions
  Evaluate the objective function
  Update the best position of each crow
end while

B. Self-Adaptive Modified Crow Search Algorithm (SAMCSA)

1) Improved Awareness Probability: In the standard CSA, by reducing the AP value, the algorithm performs a search in a local area, which leads to finding an optimal solution in that area. On the other hand, if the AP value increases, the algorithm performs a global, exhaustive search. The awareness probability parameter in the standard CSA is a fixed number. However, if the AP value remains constant in the optimization process, it may not produce the desired results. In fact, by changing the AP value to the improved awareness probability, denoted by IAP, the ratio between diversification and intensification can be controlled. In this paper, crow j and crow i use external memory and the IAP parameter is set according to this memory. In this setting, if crow j has a better response to the objective function (better memory), crow i should have a better chance of chasing it. As a result, the IAP can be formulated as

$$IAP_{j,it} = \frac{\sum_{k=1}^{4} \mu f_{i,k}^{b}}{\sum_{k=1}^{4} \mu f_{j,k}^{it}} . r_{av} + \left(1 - \frac{it}{it_{\max}}\right), \quad (41)$$

where r_{av} is a random number between 0 and 1, it_{max} is the maximum number of iterations in the algorithm, and $\mu f_{i,k}^{b}$ is the best position of the crow i. Since $rand_i$ is a random number between 0 and 1, when the average of crow j's objective functions is higher than that of crow i , crow i is more likely to follow crow j.

2) Levy Distribution: Levy distribution is used in this work for the random search of each crow. Levy Flight is a powerful mathematical tool introduced by Paul Levy. In the search space, Levi's distribution is usually more efficient than a uniform random distribution [38]. First, a step size Z_i is computed using the Mantegna method [39], that is

$$Z_i = \frac{r_a}{|r_b|^{\frac{1}{\tau}}},\ r_a \sim N\left(0, \sigma_a^2\right),\ r_b \sim N\left(0, \sigma_b^2\right),$$
$$\sigma_a = \left(\frac{\Gamma\left(1+\tau\right) \times \sin\left(\pi\tau/2\right)}{\Gamma\left(1+\tau/2\right) \times \tau \times 2^{(\tau-1)/2}}\right)^{1/\tau},\ \sigma_b = 1. \quad (42)$$

Z_i is essentially a step in the random walk. Random walk is a Markov chain as the next position depends only on the current position and the transition probabilities, and the Levy flight has a long stride in iteration [40]. We can calculate the new position of crow i as

$$\mathbf{X}_i^{it} = \mathbf{X}_i^{it-1} + fl\left(\mathbf{B}_{p,i} - \mathbf{X}_i^{it-1}\right) + Z_i\left(\mathbf{X}_l^{it} - \mathbf{X}_i^{it-1}\right), \quad (43)$$

where $\mathbf{X}_l^{it}$ is a Pareto optimal solution calculated using the Roulette Wheel. The number of Pareto points is stored in an external memory called repository. Due to the limited capacity of the repository, some Pareto points are controlled by the Roulette Wheel so that the speed of the optimization algorithm is not reduced.

VI. Numerical Simulations

In this section, the performance of the proposed method is examined for two test networks. The first case is the IEEE 33-bus test system with one substations and 37 switches, with an operating voltage of 0.95 to 1.05 p.u. branch and load information, as given in [41]. The second case is the 86-bus Taiwan Power Company (TPC) with two substations, 11 feeders, and 96 switches [42]. Here, according to [14], we consider different types of consumers, i.e., industrial, commercial and residential consumers, with different demand time. In [36], their classification for the first case is given, and Table II shows the types of consumers in the second case. Moreover, in [30], the energy price is given in 24 hours. The RLs are at nodes 8, 21, 24, 29, 30, and 32 in the first case and at nodes 14, 21, 30, 33, 73, and 81 in the second case. Under the agreement, the DSM can control up to $\eta_l = 50$ of consumption during hours 9 to 24. Also, the DSM must pay \$115 per MWh under the contract.

In the first case, we assume that there are three renewable farms (solar generators) at nodes 9, 16, and 31, and in the second case, there are five renewable farms at nodes 15, 20, 62, 71, and 85. Historical data (mean and standard deviation) of solar radiation for 1MW PVs are given in [34]. Their features are listed in Table III [43]. Two DGs with capacities of 1MW and 0.8MW are located at nodes 15 and 25 of the first case and 8 and 55 of the second case. Also, two ESSs are located at nodes 9 and 16 in the first case and 15 and 85 in the second case. Their features are listed in Table IV [30] and Table V [32].

Each switch can participate in up to 4 switching operations a day for the purpose of reconfiguration, and none of them can be remotely controlled. The cost of each switching is estimated at \$1 [30]. In the proposed method, the distribution system operator calculates the configuration of each hour for the next 24 hours according to the announced information of the status of the renewable farm (available or not available) and the historical data of solar radiation.

Table II: demand patterns of each load point in the second case

Demand pattern	Node
Residential	1 2 3 4 5 6 7 8 9 10 11 12 13 14 15 16 17 18 19 20 21 22 23 24 25 26 27 47 48 49 50 51 52 66 67 68 69 78 79 80
Commercial	28 29 30 31 32 33 34 35 36 37 38 39 40 41 42 43 44 45 46 70 71 72 73 74 75 76 77
Industrial	53 54 55 56 57 58 59 60 61 62 63 64 65 81 82 83 84 85

Table III: The PV characteristics

PV			
T_{at}	30 (°C)	Vmp	18 (V)
I_{mp}	11.12 (A)	γ	1000
V_{oc}	22.30 (V)	M	5
I_{sc}	11.89 (A)	P_{rate}	200 (W)
K_{vt}	0.38 $(\%A)$	failure rate	6 (f/yr)
K_{et}	0.1 $(\%A)$	repair rate	144 (r/yr)

The failure rate in the branches is assumed to be proportional to the length of each of them. Since the impedance also increases with increasing the length of the line, we assume that the branch with the highest impedance has a failure rate of 0.5 $f/year$ and the branch with the lowest impedance has a failure rate of 0.1 $f/year$. The failure rate of other branches is calculated according to their impedance in proportion to these two linear values [44]. Also, the cost of PVs is assumed to be negligible.

A. Investigating the Effect of Renewable Farm Failure

As explained previously, one of the most important parameters in DNR is equipment availability. In other words, failure of any equipment item must be taken into consideration when choosing the hourly configuration. Table VI shows the probability of the number of available equipment items for a renewable source at $\triangle t = 15$. We select π_{av}^{15} with the highest probability as the number of available PV farms' equipment items. In the simulations, three scenarios are defined to investigate the effect of considering solar farm failure:

Table IV: Cost coefficients and technical data for DG units

	a_g	b_g	c_g	Su_g	Sd_g	$P_{g,\max}$ (KW)	$P_{g,\min}$ (KW)
DG1	27	79	0.0035	15	10	1000	100
DG2	25	87	0.0045	15	10	800	80

Table V: The ESS unit characteristics [32]

ESS			
$C_{\max}$ (KW/h)	300	C_{rep}(\$)	900
$SOC_{\min}$ (KW/h)	%26.6 $\times$ $C_{\max}$	N_{es}	40
P_{es}^{-} (KW/h)	-40	$Q_{\text{lifetime}}(KW/h)$	10.569
P_{es}^{+} (KW/h)	40	η_{es}	% 95

Table VI: Probability of the number of equipment items available for a PV farm at $T = 5$ and $\triangle t = 15$

A	π_{av}^{15}	A	π_{av}^{15}
0	$\pi_5^* = 0.9555$ $\pi_4^* = 0.0445$	3	$\pi_3^* = 0.7328$ $\pi_4^* = 0.2672$
1	$\pi_4^* = 0.6385$ $\pi_5^* = 0.3615$	4	$\pi_2^* = 0.6663$ $\pi_3^* = 0.3337$
2	$\pi_4^* = 0.5417$ $\pi_3^* = 0.4583$	5	$\pi_2^* = 0.7253$ $\pi_1^* = 0.2747$

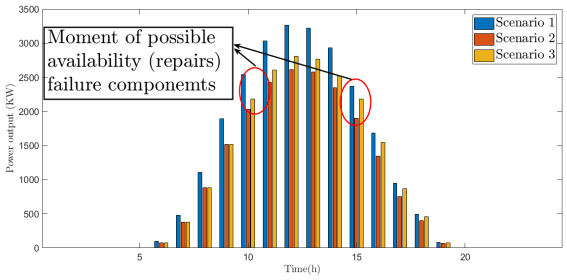

Figure 4: The sum of the power output of five PVs for the three scenarios in the second case.

- **Scenario 1:** All PV farms' equipment items are available.
- **Scenario 2:** The failure of PV farms' equipment is considered. However, it is assumed that equipment items will never be repaired or become available again.
- **Scenario 3:** The possibility of failure and the possibility of repairing PV farms are explicitly considered.

For Scenarios 2 and 3, in the first case, $A_1 = A_2 = 0$ and $A_3 = 3$, and in the second case, $A_1 = A_2 = A_3 = 0$, $A_4 = 2$, and $A_5 = 3$. Figure 4 shows the sum of five renewable farms' output power in the second case for the three scenarios with a constant amount of solar radiation. As shown in Figure 4, the power output of the renewables in Scenario 1 in the early hours of the day is much higher than in the other scenarios. Table VII provides the optimal configuration for the second case at $\triangle t = 10$ for Scenarios 1 and 3. Voltage profile for the configuration selected in Scenario 1 and 3 are demonstrated in Figure 5. It can be seen that the configuration chosen in Scenario 3 is much more appropriate.

Figure 6 shows the changes in $OF2$ given Scenarios 2 and 3 in the first case. Since in Scenario 2, the possibility of repairing the damaged components is not considered, the active power loss in this scenario has increased compared to Scenario 3.

Table VII: Open switches in the second case for Scenario 1 and 3 at $\triangle t = 10$

Scenario	Open switches						
Scenario 1	s18	s35	s46	s60	s62	s70	s76
	s81	s84	s86	s90	s92	s95	
Scenario 3	s38	s46	s53	s60	s61	s70	s83
	s88	s89	s86	s90	s92	s95	

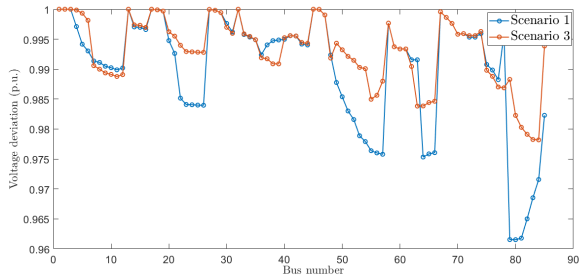

Figure 5: Voltage profile for the second case at $\triangle t = 10$

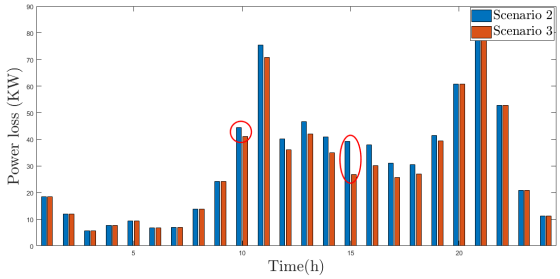

Figure 6: Active power loss for Scenarios 2 and 3 in the first case.

Figure 7 shows the operation costs for Scenarios 2 and 3 in the first case. The total OF_4 in 24 hours for Scenario 3 is \$4467.8 and for Scenario 2 is \$4660.8.

B. Comparison of SAMCSA with Other Methods

To evaluate the SAMCSA, we perform optimization with GA, PSO, and CSA algorithms at $\triangle t = 10$ for the second case given Scenario 3. The experiments are repeated 10 times and the results are presented in Table IX. The proposed SAMCSA returns superior results for the mean values of the optimal solutions, the standard deviation of optimal solutions, and the computation time compared to other methods. Also, Table VIII shows the values of the three objective functions (OF_1, OF_2, and OF_3) before reconfiguration and after reconfiguration without considering PVs, DGs, ESSs, RLs. These results show that this DNR method can be adopted as an effective strategy to improve the performance.

For ease of reviewing the values of the objective functions, the 3-D diagrams are depicted in Figure 8. Each circle in

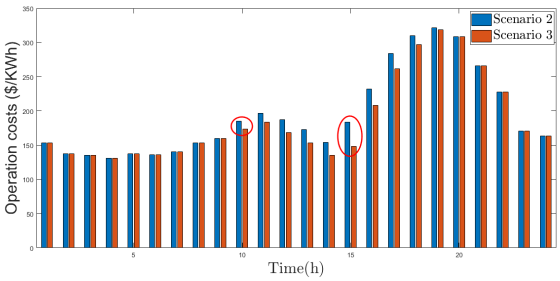

Figure 7: Operation costs for Scenarios 2 and 3 in the first case.

Table VIII: Effects of DNR at $\triangle t = 10$ on the three objective functions in the second case.

Objective functions	**Before DNR**	**After DNR**
OF_1	35.0360	26.7110
OF_2	239.6571	109.5479
OF_3	0.0446	0.0295
Open switch	s85 s86 s87 s88 s89 s90 s91 s92 s93 s94 s95 s96 s97	s96 s76 s59 s32 s14 s86 s94 s71 s92 s80 s90 s95 s55

Table IX: comparison of performance between GA, PSO, CSA and SAMCSA

Method	**Average time (min)**	**Objective function**	**Average**	**Standard deviation**
GA [20]	21.78	OF_1	39.6874	6.1365
		OF_2	141.7874	19.1785
		OF_3	0.0512	0.0446
		OF_4	1412.9	58.0346
PSO [18]	17.45	OF_1	35.2787	4.8764
		OF_2	135.4701	15.9674
		OF_3	0.0485	0.0209
		OF_4	1387.3	46.2473
CSA [37]	17.05	OF_1	32.8751	5.4565
		OF_2	128.2087	16.4972
		OF_3	0.0427	0.0475
		OF_4	1390.7	51.5794
SAMCSA	15.88	OF_1	25.7568	2.0436
		OF_2	116.3955	9.1772
		OF_3	0.0389	0.0151
		OF_4	1314.1	29.1474

the figure is a Pareto solution and in each diagram one of the objective functions is ignored. The optimal values of the objective functions are marked in cyan (reliability), red (active losses), blue (voltage deviation), and green (operation costs). As mentioned in Section IV, the values obtained from the Pareto set are generated in the random space, all of which are Pareto non-dominated responses. Also, Figure 9 shows the number of iterations required to reach convergence for OF_4 by comparing different methods in the second case.

To demonstrate the performance of the proposed method, we examine the first case without considering PVs, DGs, ESSs, RLs, and with a definite amount in the active and reactive power consumption. Table X shows the reconfiguration results with the proposed method and other methods regarding OF_2. It can be seen that the SAMCSA results are similar to those of other known methods.

VII. Conclusion

Given the high computational complexity of distribution network reconfiguration (DNR), it is difficult to take into consideration many issues such as equipment failure when performing DNR. In this paper, the possibility of failure of renewable resources is considered, leading to the so-called SDNR method. In this method, the number of scenarios is reduced using the probability distance method, then the

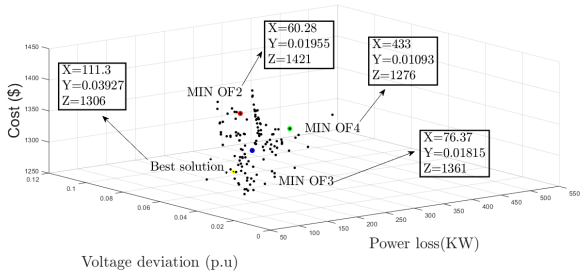

(a) Objective functions except OF_1.

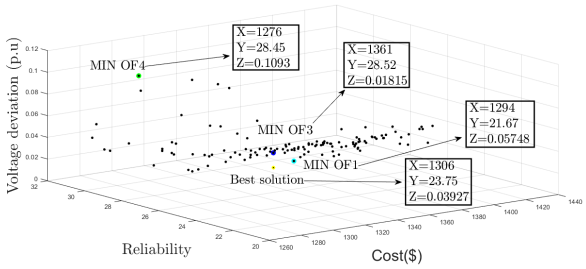

(b) Objective functions except OF_2.

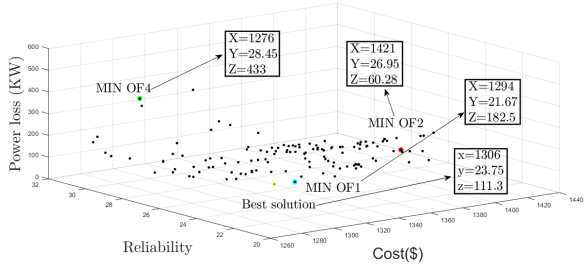

(c) Objective functions except OF_3.

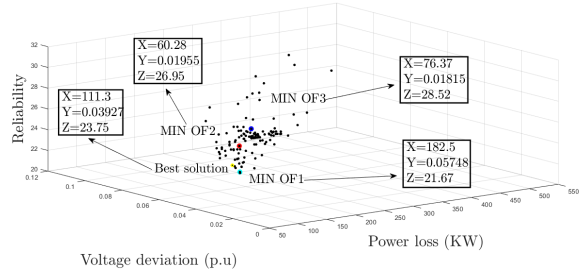

(d) Objective functions except OF_4.

Figure 8: 3-D plot of the non-dominated solutions investigating objective functions in the second case at $\triangle t = 10$.

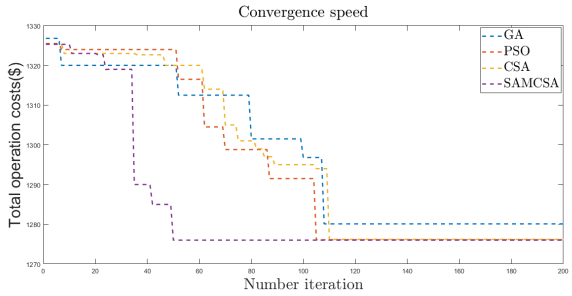

Figure 9: Single line comparing the convergence speed of the SAMCSA with those of other methods of operation costs in the second case.

Table X: Comparison with respect to OF_2 of the proposed method with other methods in the first case

Method	**Power loss (KW)**	**Open switches**
Vanderson Gomes [3]	139.53	s7,s9,s14,s32,s37
MBA [19]	139.53	s7,s9,s14,s32,s37
MHBMO , DPSO [45]	139.53	s7,s9,s14,s32,s37
Goswami [46]	143.69	s7,s9,s14,s32,s37
PSO-ACO [47]	139.53	s7,s9,s14,s32,s37
SAMCSA	139.53	s7,s9,s14,s32,s37

best scenario is selected. The SAMCSA algorithm has also been proposed to solve the DNR problem efficiently. The performance of this algorithm has been compared with the GA and PSO algorithms in terms of computation time. Given the promising reduction in computation time, this algorithm should be suitable for implementation in large-scale networks. A short list of future directions for this research includes considering dispatch DG (at the same time as DNR), optimizing critical switches, and improving search methods to find optimal solution.

REFERENCES

[1] Y. Wang, S. Zhou, and H. Huo, "Cost and co2 reductions of solar photovoltaic power generation in china: Perspectives for 2020," *Renewable and Sustainable Energy Reviews*, vol. 39, pp. 370–380, 2014.

[2] F. W. Geels, A. McMeekin, J. Mylan, and D. Southerton, "A critical appraisal of sustainable consumption and production research: The reformist, revolutionary and reconfiguration positions," *Global Environmental Change*, vol. 34, pp. 1–12, 2015.

[3] F. V. Gomes, S. Carneiro, J. L. R. Pereira, M. P. Vinagre, P. A. N. Garcia, and L. R. Araujo, "A new heuristic reconfiguration algorithm for large distribution systems," *IEEE Transactions on Power systems*, vol. 20, no. 3, pp. 1373–1378, 2005.

[4] C. Li, S. Miao, Y. Li, D. Zhang, C. Ye, Z. Liu, and L. Li, "Coordinating dynamic network reconfiguration with anm in active distribution network optimisation considering system structure security evaluation," *IET Generation, Transmission & Distribution*, vol. 13, no. 19, pp. 4355–4363, 2019.

[5] S. Chuangpishit, A. Tabesh, Z. Moradi-Shahrbabak, and M. Saeedifard, "Topology design for collector systems of offshore wind farms with pure dc power systems," *IEEE Transactions on Industrial Electronics*, vol. 61, no. 1, pp. 320–328, 2013.

[6] F. Pilo, G. Pisano, and G. G. Soma, "Optimal coordination of energy resources with a two-stage online active management," *IEEE Transactions on Industrial Electronics*, vol. 58, no. 10, pp. 4526–4537, 2011.

[7] N. G. Paterakis, A. Mazza, S. F. Santos, O. Erdinç, G. Chicco, A. G. Bakirtzis, and J. P. Catalão, "Multi-objective reconfiguration of radial distribution systems using reliability indices," *IEEE Transactions on Power Systems*, vol. 31, no. 2, pp. 1048–1062, 2015.

[8] M. T. G. Jahani, P. Nazarian, A. Safari, and M. Haghifam, "Multi-objective optimization model for optimal reconfiguration of distribution networks with demand response services," *Sustainable Cities and Society*, vol. 47, p. 101514, 2019.

[9] M.-R. Andervazh, J. Olamaei, and M.-R. Haghifam, "Adaptive multi-objective distribution network reconfiguration using multi-objective discrete particles swarm optimisation algorithm and graph theory," *IET Generation, Transmission & Distribution*, vol. 7, no. 12, pp. 1367–1382, 2013.

[10] S. Mishra, D. Das, and S. Paul, "A comprehensive review on power distribution network reconfiguration," *Energy Systems*, vol. 8, no. 2, pp. 227–284, 2017.

[11] A. Abbaskhani-Davanloo, M. Amini, M. S. Modarresi, and F. Jafarishiadeh, "Distribution system reconfiguration for loss reduction incorporating load and renewable generation uncertainties," in *2019 IEEE Texas Power and Energy Conference (TPEC)*. IEEE, 2019, pp. 1–6.

[12] A. Azizivahed, A. Arefi, S. Ghavidel, M. Shafie-khah, L. Li, J. Zhang, and J. P. Catalão, "Energy management strategy in dynamic distribution network reconfiguration considering renewable energy resources and storage," *IEEE Transactions on Sustainable Energy*, vol. 11, no. 2, pp. 662–673, 2019.

[13] Y.-Y. Fu and H.-D. Chiang, "Toward optimal multiperiod network reconfiguration for increasing the hosting capacity of distribution networks," *IEEE Transactions on Power Delivery*, vol. 33, no. 5, pp. 2294–2304, 2018.

[14] E. Lopez, H. Opazo, L. Garcia, and P. Bastard, "Online reconfiguration considering variability demand: Applications to real networks," *IEEE Transactions on Power systems*, vol. 19, no. 1, pp. 549–553, 2004.

[15] C.-S. Chen, C.-H. Lin, H.-J. Chuang, C.-S. Li, M.-Y. Huang, and C.-W. Huang, "Optimal placement of line switches for distribution automation systems using immune algorithm," *IEEE Transactions on Power Systems*, vol. 21, no. 3, pp. 1209–1217, 2006.

[16] Z. Guo, Z. Zhou, and Y. Zhou, "Impacts of integrating topology reconfiguration and vehicle-to-grid technologies on distribution system operation," *IEEE Transactions on Sustainable Energy*, vol. 11, no. 2, pp. 1023–1032, 2019.

[17] F. Capitanescu, L. F. Ochoa, H. Margossian, and N. D. Hatziargyriou, "Assessing the potential of network reconfiguration to improve distributed generation hosting capacity in active distribution systems," *IEEE Transactions on Power Systems*, vol. 30, no. 1, pp. 346–356, 2014.

[18] S. M. M. Larimi, M. R. Haghifam, and A. Moradkhani, "Risk-based reconfiguration of active electric distribution networks," *IET Generation, Transmission & Distribution*, vol. 10, no. 4, pp. 1006–1015, 2016.

[19] A. Kavousi-Fard and T. Niknam, "Multi-objective stochastic distribution feeder reconfiguration from the reliability point of view," *Energy*, vol. 64, pp. 342–354, 2014.

[20] F. Ding and K. A. Loparo, "Feeder reconfiguration for unbalanced distribution systems with distributed generation: A hierarchical decentralized approach," *IEEE Transactions on Power Systems*, vol. 31, no. 2, pp. 1633–1642, 2015.

[21] H. Haghighat and B. Zeng, "Distribution system reconfiguration under uncertain load and renewable generation," *IEEE Transactions on Power Systems*, vol. 31, no. 4, pp. 2666–2675, 2015.

[22] S. Lei, Y. Hou, F. Qiu, and J. Yan, "Identification of critical switches for integrating renewable distributed generation by dynamic network reconfiguration," *IEEE Transactions on Sustainable Energy*, vol. 9, no. 1, pp. 420–432, 2017.

[23] A. Borghetti, "A mixed-integer linear programming approach for the computation of the minimum-losses radial configuration of electrical distribution networks," *IEEE Transactions on Power Systems*, vol. 27, no. 3, pp. 1264–1273, 2012.

[24] R. A. Jabr, R. Singh, and B. C. Pal, "Minimum loss network reconfiguration using mixed-integer convex programming," *IEEE Transactions on Power systems*, vol. 27, no. 2, pp. 1106–1115, 2012.

[25] E. Romero-Ramos, J. Riquelme-Santos, and J. Reyes, "A simpler and exact mathematical model for the computation of the minimal power losses tree," *Electric Power Systems Research*, vol. 80, no. 5, pp. 562–571, 2010.

[26] R. S. Rao, K. Ravindra, K. Satish, and S. Narasimham, "Power loss minimization in distribution system using network reconfiguration in the presence of distributed generation," *IEEE Transactions on Power Systems*, vol. 28, no. 1, pp. 317–325, 2012.

[27] A. R. Malekpour, T. Niknam, A. Pahwa, and A. K. Fard, "Multi-objective stochastic distribution feeder reconfiguration in systems with wind power generators and fuel cells using the point estimate method," *IEEE Transactions on Power Systems*, vol. 28, no. 2, pp. 1483–1492, 2012.

[28] A. J. Conejo, M. Carrión, J. M. Morales *et al.*, *Decision making under uncertainty in electricity markets*. Springer, 2010, vol. 1.

[29] R. Jabbari-Sabet, S.-M. Moghaddas-Tafreshi, and S.-S. Mirhoseini, "Microgrid operation and management using probabilistic reconfiguration and unit commitment," *International Journal of Electrical Power & Energy Systems*, vol. 75, pp. 328–336, 2016.

[30] S. Golshannavaz, S. Afsharnia, and F. Aminifar, "Smart distribution grid: Optimal day-ahead scheduling with reconfigurable topology," *IEEE Transactions on Smart Grid*, vol. 5, no. 5, pp. 2402–2411, 2014.

[31] S. Esmaeili, A. Anvari-Moghaddam, S. Jadid, and J. M. Guerrero, "Optimal simultaneous day-ahead scheduling and hourly reconfiguration of distribution systems considering responsive loads," *International Journal of Electrical Power & Energy Systems*, vol. 104, pp. 537–548, 2019.

[32] V. S. Tabar, M. A. Jirdehi, and R. Hemmati, "Energy management in microgrid based on the multi objective stochastic programming incorporating portable renewable energy resource as demand response option," *Energy*, vol. 118, pp. 827–839, 2017.

[33] A. Moshari, A. Ebrahimi, and M. Fotuhi-Firuzabad, "Short-term impacts of dr programs on reliability of wind integrated power systems considering demand-side uncertainties," *IEEE Transactions on Power Systems*, vol. 31, no. 3, pp. 2481–2490, 2015.

[34] M. Mazidi, A. Zakariazadeh, S. Jadid, and P. Siano, "Integrated scheduling of renewable generation and demand response programs in a microgrid," *Energy Conversion and Management*, vol. 86, pp. 1118–1127, 2014.

[35] Y. Atwa, E. El-Saadany, M. Salama, and R. Seethapathy, "Optimal renewable resources mix for distribution system energy loss minimization," *IEEE Transactions on Power Systems*, vol. 25, no. 1, pp. 360–370, 2009.

[36] D. Q. Hung, N. Mithulananthan, and K. Y. Lee, "Determining pv penetration for distribution systems with time-varying load models," *IEEE Transactions on Power Systems*, vol. 29, no. 6, pp. 3048–3057, 2014.

[37] A. Askarzadeh, "A novel metaheuristic method for solving constrained engineering optimization problems: crow search algorithm," *Computers & Structures*, vol. 169, pp. 1–12, 2016.

[38] M. Jain, A. Rani, and V. Singh, "An improved crow search algorithm for high-dimensional problems," *Journal of Intelligent & Fuzzy Systems*, vol. 33, no. 6, pp. 3597–3614, 2017.

[39] P. Díaz, M. Pérez-Cisneros, E. Cuevas, O. Avalos, J. Gálvez, S. Hinojosa, and D. Zaldivar, "An improved crow search algorithm applied to energy problems," *Energies*, vol. 11, no. 3, p. 571, 2018.

[40] X.-S. Yang and S. Deb, "Cuckoo search via lévy flights," in *2009 World congress on nature & biologically inspired computing (NaBIC)*. IEEE, 2009, pp. 210–214.

[41] M. E. Baran and F. F. Wu, "Network reconfiguration in distribution systems for loss reduction and load balancing," *IEEE Power Engineering Review*, vol. 9, no. 4, pp. 101–102, 1989.

[42] J.-P. Chiou, C.-F. Chang, and C.-T. Su, "Variable scaling hybrid differential evolution for solving network reconfiguration of distribution systems," *IEEE Transactions on Power Systems*, vol. 20, no. 2, pp. 668–674, 2005.

[43] T. Adefarati and R. Bansal, "Reliability assessment of distribution system with the integration of renewable distributed generation," *Applied Energy*, vol. 185, pp. 158–171, 2017.

[44] A. Etemadi and M. Fotuhi-Firuzabad, "Distribution system reliability enhancement using optimal capacitor placement," *IET Generation, Transmission & Distribution*, vol. 2, no. 5, pp. 621–631, 2008.

[45] T. Niknam, "An efficient hybrid evolutionary algorithm based on pso and aco for distribution feeder reconfiguration," *European Transactions on Electrical Power*, vol. 20, no. 5, pp. 575–590, 2010.

[46] S. K. Goswami and S. K. Basu, "A new algorithm for the reconfiguration of distribution feeders for loss minimization," *IEEE Transactions on Power Delivery*, vol. 7, no. 3, pp. 1484–1491, 1992.

[47] A. Kavousi-Fard and T. Niknam, "Considering uncertainty in the multi-objective stochastic capacitor allocation problem using a novel self adaptive modification approach," *Electric Power Systems Research*, vol. 103, pp. 16–27, 2013.